

Green Chemistry

Accepted Manuscript



This article can be cited before page numbers have been issued, to do this please use: J. He, M. Liu, K. Huang, T. W. Walker, C. T. Maravelias, J. A. Dumesic and G. Huber, *Green Chem.*, 2017, DOI: 10.1039/C7GC01688C.



This is an Accepted Manuscript, which has been through the Royal Society of Chemistry peer review process and has been accepted for publication.

Accepted Manuscripts are published online shortly after acceptance, before technical editing, formatting and proof reading. Using this free service, authors can make their results available to the community, in citable form, before we publish the edited article. We will replace this Accepted Manuscript with the edited and formatted Advance Article as soon as it is available.

You can find more information about Accepted Manuscripts in the [author guidelines](#).

Please note that technical editing may introduce minor changes to the text and/or graphics, which may alter content. The journal's standard [Terms & Conditions](#) and the ethical guidelines, outlined in our [author and reviewer resource centre](#), still apply. In no event shall the Royal Society of Chemistry be held responsible for any errors or omissions in this Accepted Manuscript or any consequences arising from the use of any information it contains.

Production of levoglucosenone and 5-hydroxymethylfurfural from cellulose in polar aprotic solvent-water mixtures

Jiayue He, Mingjie Liu, Kefeng Huang, Theodore W. Walker, Christos T. Maravelias, James A. Dumesic and George W. Huber*

Department of Chemical and Biological Engineering, University of Wisconsin-Madison, Madison, WI 53706, USA.

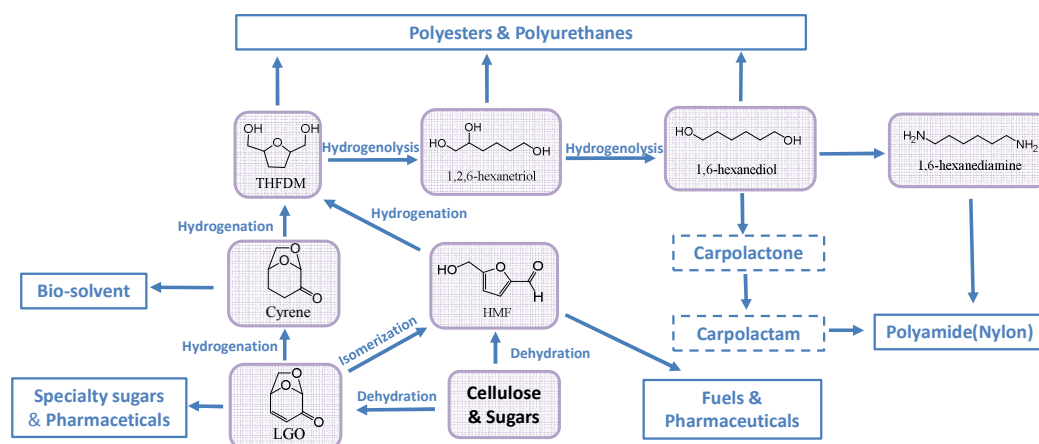
*Correspondence to: gwhuber@wisc.edu

Abstract

We demonstrate a process to produce levoglucosenone (LGO) and 5-hydroxymethylfurfural (HMF) from cellulose in up to 65% carbon yield using sulfuric acid as catalyst and a solvent consisting of a mixture of tetrahydrofuran (THF) with water. In pure THF, LGO is the major product of cellulose dehydration, passing through levoglucosan as an intermediate. Increasing the water content (up to 5 wt%) results in HMF as the major product. HMF is formed both by glucose dehydration and direct dehydration of LGA. The maximum combined yield of LGO and HMF (~65 carbon %) is achieved in the presence of 1 - 2.5 wt% H₂O, such that comparable amounts of these two co-products are formed. THF gave the highest total yields of LGO and HMF among the solvents investigated in this study (i.e., THF, diglyme, tetraglyme, GVL, CPME, dioxane, and DMSO). Furthermore, the rate of LGO and HMF degradation in THF was lower than in the other solvents. LGO/HMF yields increased with increased strength of the acid catalyst (H₂SO₄ > H₃PO₄ > HCOOH), and HMF was produced more selectively than LGO in the presence of hydrochloric acid. Techno-economic analysis for LGO and HMF production from cellulose shows that the lowest LGO/HMF production costs are less than \$3.50/kg and occur at cellulose loading and water content of 1%~3% and 0~5% respectively.

Introduction

Cellulose, the most abundant organic polymer in nature, has been used as a renewable nonpetroleum feedstock to produce important chemical precursors, including levoglucosenone (LGO)^{1–14} and 5-hydroxymethylfurfural (HMF)^{15–26}. Both LGO and HMF can be used as building blocks for the production of various high-volume organic chemicals with numerous industrial applications, as shown in **Scheme 1**. HMF (a product of cellulose dehydration) is a precursor for pharmaceuticals, plastics, and fuels applications. HMF is also produced by the isomerization of LGO²⁷. The chiral nature of LGO (another product of cellulose dehydration) makes it a natural synthon for products containing C-glycosides,²⁸ which are naturally occurring derivatives and components of important compounds from the flavone, chromone, xanthone, anthrone, and gallic acid groups.^{29,30} LGO can be hydrogenated to cyrene²⁷, a green solvent that has been reported as a replacement for N-Methyl-2-pyrrolidone (NMP) and dimethylformamide (DMF).³¹ Polyhydric alcohols, including tetrahydrofuran-dimethanol (THFDM), 1,2,6-hexanetriol and 1,6-hexanediol, can be produced from both LGO and HMF. 1,6-hexanediol is used in the production of polyesters and polyurethanes.³² THFDM can be used as a diol in the preparation of polyesters.³³ 1,2,6-hexanetriol, as a polyhydric alcohol, can be used as cross-linker in the production of polyesters and alkyd resins.^{34,35}



Scheme 1 The potential applications of LGO and HMF derived from cellulose/sugars.

Production of HMF from cellulose in aqueous solutions only occurs in low yields (less than 8%) because of the formation humins^{36–38}. HMF is produced in higher yields from fructose dehydration (e.g., 72%).²¹ In a monophasic solvent system, HMF forms condensation products with fructose, meaning that dilute feedstocks must be used.³⁸ HMF can be produced from glucose in a biphasic water-alkylphenol solvent through a two-step process consisting of: a) isomerization of glucose to fructose over AlCl_3 ; and b) dehydration of fructose over HCl to form HMF in a yield of 62%.³⁹ We have previously demonstrated that a mixture of HMF and LGO can be produced from cellulose in 44% carbon yield (all yields in this paper are on a carbon basis), in a THF solvent in the presence of 5 mM H_2SO_4 .^{10,17} Atanda et al. reported the

transformation of cellulose derived complex sugars (mechanocatalytic depolymerized cellulose) to HMF in high yields (74.7-86%) using a POx-TiO₂ catalyst in a H₂O-THF system containing N-methyl-2-pyrrolidone (NMP). The cellulose-derived complex sugars were prepared by ball milling of acid-impregnated cellulose.^{22,23} Cai *et al.* were able to produce HMF from maple wood in up to 51% yield using FeCl₃ with a THF-H₂O solvent.^{40,41} Their study revealed how the interplay between relative Brønsted and Lewis acidities was responsible for enhancing catalytic performance in THF co-solvent. However, the introduction of chloride requires reactors made from corrosion-resistant materials, as steels undergo pitting from chlorides.⁴² Alternatively, this approach would require a novel separation technology to remove the iron chloride. In a H₂O-THF solvent system, Xia *et al.* used a FePO₄ catalyst to produce HMF from cellulose in yields up to 37.9 mol%.¹⁹ The soluble iron species, such as Fe³⁺ species, act as Lewis acid sites catalyzing isomerization of cellulose-derived glucose to fructose followed by the dehydration of fructose into HMF catalyzed by protons.

High yields of HMF from cellulose can also be obtained in ionic liquids due to their ability to fully solubilize raw cellulose.²⁴⁻²⁶ For example, Zhang and co-workers have reported HMF yields of 55% from cellulose with a mixture of CuCl₂/CrCl₂ dissolved in 1-ethyl-3-methylimidazolium ([EMIM]Cl).^{26,43} However, it is difficult to separate the products from the ionic liquids, which limits their commercial viability. Although the production of HMF from cellulose in mixtures of water with polar aprotic co-solvents has been studied, especially the H₂O-THF system, no systematic study has been conducted to evaluate how the water concentration and cellulose loading (1-10 wt.%) influence yields, selectivities, and process economics.

In contrast to HMF, LGO production in condensed-phase process schemes has received relatively little attention. Several papers have described approaches to produce LGO from cellulose *via* pyrolysis techniques that often involve several solvents⁷. However, these pyrolysis approaches produce low yields of LGO.^{2-5,8,12-14} For example, pyrolysis of acid-pretreated cellulose produced LGO in 34% yield.¹ LGO yields below 8% have been reported with microwave-assisted pyrolysis.^{5,6,11} Vacuum pyrolysis (0.1 atm) has demonstrated LGO and HMF yields as high as 42.2% and 8.8% (on a carbon basis, respectively) in sulfolane solvent.⁹ LGO has been produced in low yields from raw biomass pyrolysis with solid acids (CeO₂, Nb₂O₅, Al-Fe-MCM-48)⁵ (LGO yield <10%), solid acids including sulfonated zirconia⁸ (LGO yield <10%), SO₄²⁻/TiO₂ (LGO yield ~14.9%)^{4,13} and SO₄²⁻/TiO₂-Fe₃O₄ (LGO yield ~ 15.4%)⁴. Sulfonated ionic liquids² and 1-butyl-2,3-dimethylimidazolium triflate³ have also been employed in solvent-assisted cellulose pyrolysis, but the highest yield of LGO was less than 30% in ionic liquids. Previously, we have shown that LGO can be produced in approximately 50% yield from cellulose, under mild reaction conditions, using polar aprotic solvents and an inexpensive sulfuric acid catalyst.¹⁰ However, these experiments were done with 1 wt% cellulose in THF. Also, the reaction kinetics, impact of water content on the reaction pathway, and the influence of cellulose loadings were not explored in detail.

The lowest HMF production costs in the literature all use fructose as a feedstock⁴⁴⁻⁴⁹, at a predicted cost of \$1.00/kg in large scale processes.^{50,51} It has also

been reported that HMF could economically be produced from cellulose from lignocellulose feedstocks at scales sizes of over 100 kton/yr.⁵¹ LGO is currently 70,000 times more valuable than ethanol.¹¹

The objective of this study is to study the role of cellulose loading and water content in THF-H₂O mixtures on the reaction pathway for LGO and HMF production. We also investigate the effect of various polar aprotic solvents and mineral acids on the production of HMF and/or LGO from cellulose. In addition, techno-economic analyses are carried out to demonstrate optimal process conditions for LGO and HMF co-production from cellulose, as expressed by a minimization in overall production cost.

Experimental

Dehydration reactions

Reactions were carried out in a 100 mL autoclave (Parr Instrument Company, series 4560, Hastelloy (C-276)). The vessel and head were dried overnight at 70 °C to remove residual water prior to each reaction. The reagents, including cellulose (Avicel[®] PH-101, moisture content ca. 3 wt%), glucose (Sigma Aldrich, anhydrous), LGA (TCI, purity 99%), THF (Acros, anhydrous, 99.9%, stabilized with BHT), and sulfuric acid (Fisher Chemical, A300-500), were used as received. Reactants, solvent, and sulfuric acid were added to the autoclave sequentially, at which point the vessel was purged five times with helium (99.999%, Airgas) and charged to 3.4 MPa He. The vessel was then heated to the desired reaction temperature and pressurized with He to a final pressure of 1000 psi. Zero time was defined as the point at which the heating was started, except where noted. The temperature and stirring were maintained at 700 rpm and controlled by a Parr 4848 Controller. Around 1 mL samples were taken periodically through a dip tube during the reaction. The reactor was re-pressurized with helium to 1000 psi after each sampling. The samples were quenched in a dry ice bath and then filtered with a 0.22 μm syringe filter (Restek, PTFE (polytetrafluoroethylene)) prior to the analysis.

Analytical methods

LGO (Standards, Apollo Scientific, purity 98%) and HMF (Standards, Sigma Aldrich, purity >99%) were analyzed using a high-performance liquid chromatograph (HPLC; Shimadzu, LC-20AT) equipped with UV (UV-vis; SPD-20AV) and RI (RID-10A) detectors. Separation was achieved using a Biorad Aminex HPX-87H column at 30 °C with 5 mM H₂SO₄ as the mobile phase, flowing at a rate of 0.6 mL · min⁻¹. The injection volume was 1 μL in each analysis.

All carbon yields were calculated as follows, where detectable products are

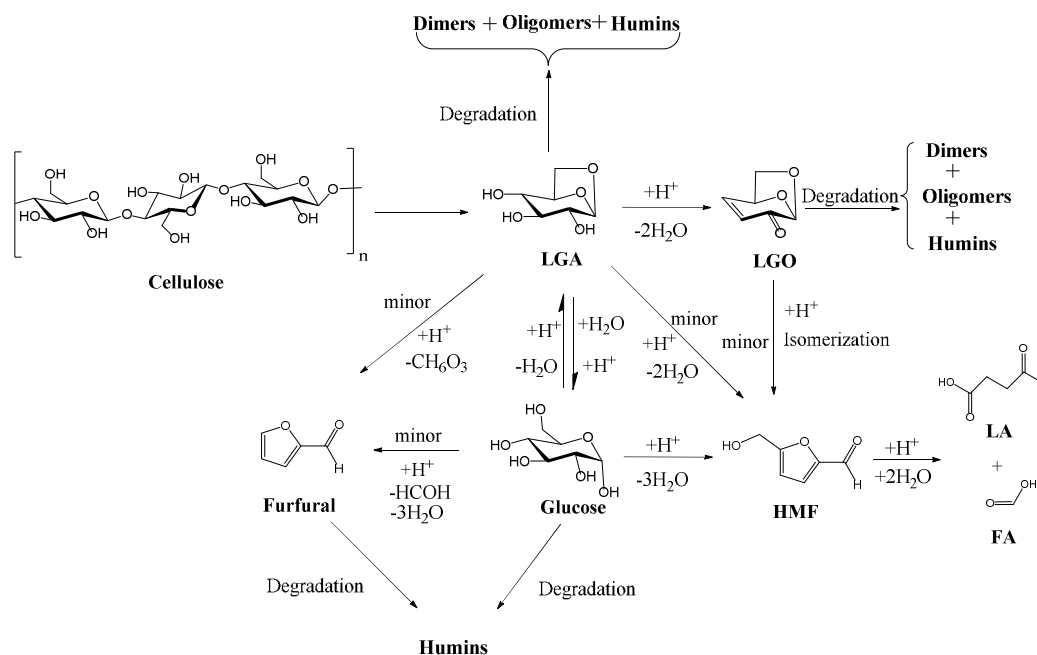
glucose, LGA, LGO, HMF, levulinic acid, formic acid, and furfural:

$$Yield_i(\%) = 100 \times \frac{\text{moles of carbon of product } i}{\text{Initial moles of carbon in feed}}$$

$$\text{overall yield } \Sigma Yield_i(\%) = 100 \times \frac{\Sigma(\text{moles of carbon of product } i)}{\text{Initial moles of carbon in feed}}$$

Results and discussions

Scheme 2 shows the proposed reaction pathway for LGO and HMF production from cellulose in mixtures of water and polar aprotic co-solvents. All reactions occur in the presence of a Brønsted-acid catalyst. Cellulose initially undergoes depolymerization to form LGA in the absence of water, or in the presence of dilute H₂O (<5 wt%) in polar aprotic solvents. LGA has also been reported as the initial product of cellulose pyrolysis.^{52,53} LGA can be dehydrated to LGO, which oligomerizes to dimers/oligomers,⁵⁴ or polymerizes to form humins. Glucose is the major secondary product formed from LGA hydration.⁵⁵ LGA can also undergo direct dehydration to form HMF,¹⁷ furfural,⁵⁶ dimers, oligomers and humins.⁵⁷ Glucose can dehydrate to HMF or form humins.⁵⁸ HMF can undergo rehydration with water over an acid catalyst to produce levulinic acid (LA) and formic acid (FA). Furfural is a minor product formed from glucose (<24% furfural yield at 120°C)⁵⁹ and/or LGA (<2% furfural yield at 170°C)⁵⁷, which also produces humins.¹⁷ As will be shown in this paper, LGO isomerization is only a minor pathway for HMF formation in THF with low concentrations of water (<5 wt%).⁶⁰



Scheme 2. Proposed reaction pathway for LGO and HMF production in the presence/absence of low concentration of water.

Polar aprotic solvent effect on cellulose dehydration

LGO and HMF are not formed from cellulose in water or in ethanol in the presence of H_2SO_4 . Conversion of cellulose in acetone and ethyl acetate also led to low yields of LGO (2-4%) and HMF (0-3%), while the use of polar aprotic solvents (THF/GVL) led to higher yields of HMF (4%) and LGO (6-15%) at 170°C in the presence of 5 mM H_2SO_4 .^{10,17} The yields of all detectable products from cellulose conversion at 210°C in different polar aprotic solvents are shown in **Table 1**. The product yields listed in **Table 1** are at the reaction time when the maximum of LGO and HMF yields were obtained. No LGO or HMF was produced in DMSO, which is likely due to the higher pKa of H_2SO_4 in this solvent,^{61,62} and that DMSO is a stronger base than water.⁶¹ DMSO has a higher polarity and dipole moment (0.444 and 4.1 D, **Table S1**) compared to the other solvents tested in this study. Another solvent with a relatively high dipole moment (5.3 D), gamma-Valerolactone (GVL) also led to low LGO (15.5%) and HMF (11.9%) yields. A major unknown product, with an estimated yield of 29.4% (if formed from cellulose) was formed directly from GVL. (**Figure S7**) We studied a series of solvents, shown in **Table S1**, with relatively lower polarities (0.164-0.224), including THF (0.207, 1.7 D), diglyme (0.224, 1.92 D), tetraglyme (0.224, 1.92 D), and 1,4-dioxane (0.164, 0.45 D). Appreciable concentrations of identifiable products are formed in these solvents. Cyclopentyl methyl ether (CPME) produced lower yields of LGO (18%) and HMF (4%) than THF, diglyme, tetraglyme and 1,4-dioxane. Solvents with moderate polarities/dipole moment, except for CPME, produced higher LGO and HMF yields. We selected a subset of polar aprotic solvents

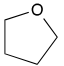
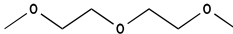
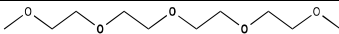
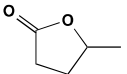
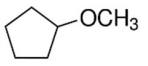
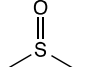
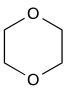
in this category (THF, diglyme, tetraglyme and dioxane) for further study.

The stability of LGO and HMF in THF, diglyme, tetraglyme and 1,4-dioxane at 210 °C was studied as shown in **Figure S4-6** and **S10**. Higher LGO yields were obtained in diglyme (42.3%), tetraglyme (38.3%) and 1,4-dioxane (39.7%) than in THF (37.5%). However, the LGO yields decreased with time more rapidly in diglyme, tetraglyme and 1,4-dioxane (to 18.6% in 155 min, 16.9% in 102 min and 8.0% in 107 min, respectively) than in THF (decreased to 35.2% in 158 minutes). Thus, the rate of LGO degradation was lower in THF than in diglyme, tetraglyme and 1,4-dioxane. Since LGO (bp = 254 °C) and HMF (bp = 292 °C) both have high boiling points, which are higher than most of the common polar aprotic solvents (**Table S1**), using a low boiling point solvent THF (bp = 66 °C) (**Table S1**) makes downstream distillation separation more energy-efficient.

Acid effect on cellulose dehydration

The effects of different acids (H₂SO₄, H₃PO₄, HCOOH and HCl) on cellulose dehydration at 210 °C with 20 mM acid in THF are shown in **Table 2**. Control measurements (without acid) with cellulose in THF resulted in negligible cellulose conversion and no detectable products at 170 °C after 6 h. The LGO/HMF yields decreased in the following order: H₂SO₄ (37.5%/10.7%) > H₃PO₄ (10.4%/10%) > HCOOH (0%/1.1%). The LGO/HMF yields generally correlate with the proton donating ability of the acid (as expressed by their pK_a values in H₂O), which decreased in the following order H₂SO₄ (pK_a = -3) > H₃PO₄ (pK_a = 2.12) > HCOOH (pK_a = 3.75). The total yields of LGO, HMF and LGA are comparable (40.7-54.9%) with HCl, H₃PO₄ and H₂SO₄ (**Table 2**). The HMF yield (19.6%) in HCl is two times higher than in H₂SO₄ (10.7%) or H₃PO₄ (10%). This result may be explained by the known role of the chloride anion in stabilizing key transition states in liquid-phase carbohydrate conversions, in particular with regards to xylose dehydration to yield furfural.⁶³⁻⁶⁵

Table 1. Maximum LGO/HMF product yields for cellulose conversion in various solvents.

Solvent	Chemical structure	Reaction time* (min.)	Yield (%)						
			LGO	HMF	LGA	Glucose	Furfural	LA	FA
THF		48	39.5	10.7	4.7	0.4	3.5	3.6	0.4
Diglyme		45	42.3	10.4	0.9	0.2	4.8	2.5	0.9
Tetraglyme		42	38.3	10.2	0	0	6.3	0.4	0.5
GVL#		30	15.5	11.9	1.8	0.3	7.5	-	0.4
CPME		40	18.0	4.1	0	0	5.4	0.5	0.9
DMSO		50	0	0	3.3	0	0	0	0
1,4-dioxane ^g		47	39.7	11.5	0	0	5.2	2.0	0.4

Reaction conditions: Cellulose (1 wt%), Solvent (60 mL), H₂SO₄ (64 μL Conc., 20 mM), 1000 psi He, 210 °C, 700 rpm. * The reaction time for maximum yield of LGO and HMF. #A major unknown product with a yield of 29.4% is afforded in GVL.

Table 2. Effect of acid on cellulose dehydration in THF

Acid	Reaction Time* (min.)	Yield (wt%)								
		LGO	HMF	LGA	Glucose	Furfural	LA	FA	LGO and HMF	LGO, HMF and LGA
H ₂ SO ₄ ^a	48	37.5	10.7	4.7	0.4	3.5	3.6	0.4	48.1	54.9
H ₃ PO ₄ ^b	160	10.4	10	20.5	0.3	0	1.0	0.3	20.4	40.9
HCOOH ^c	154	0	1.1	0.5	0	0.1	0	0	1.1	1.6
HCl ^d	170	5.3	19.6	15.8	1.9	3.4	0	0	24.9	40.7

Reaction conditions: Cellulose (1 wt%), THF (60 mL), acid (20 mM), 1000 psi He, 210 °C, 700 rpm. * The reaction time for highest yield of LGO and HMF.

Role of water on the reaction pathway

Figure 1 shows the reaction profiles versus time for cellulose and LGA conversion in pure THF, and in THF with 1 wt% H₂O at 170°C with 7.5 mM H₂SO₄. Cellulose initially undergoes anhydrous depolymerization to form LGA. The LGA yield increases to a maximum of 23.4% at 40 min in pure THF and then gradually decreases to 11.4% in 90 min, as shown in **Fig 1a**. LGO and HMF yields increase during the entire 90 min time course, suggesting that they are both formed from LGA. There is only a small amount of glucose (< 0.3%) observed during the first 90 mins. A control experiment for LGO conversion was performed in pure THF at 170°C with 7.5 mM H₂SO₄. A 0.5 % HMF yield was obtained with 25% LGO conversion. Thus, formation of HMF from LGO conversion is only a minor reaction pathway in pure THF.

According to **Figure 1b**, the primary product from cellulose conversion is LGA in THF/H₂O (99/1) mixture. The LGA goes through a maximum of 26.5% yield at 45 mins and then decreases at longer residence times. The LGO yield is lower and the HMF yield is higher in the THF/H₂O (99/1) mixture than in the pure THF. The glucose yield (5.2% yield in 30 mins) is also higher in this solvent mixture. The HMF yield from cellulose increased from 11.4% in 90 mins in pure THF to 25.3% in the THF/H₂O (99/1) solvent. The LGA conversion profile versus time in pure THF at 170°C with 7.5 mM H₂SO₄ is shown in **Figure 1c**. LGA is converted to both LGO (31.5% yield in 90 mins) and HMF (5.5% yield in 90 mins.). The LGA conversion versus time behavior in THF/H₂O (99/1) mixture is shown in **Figure 1d**. The 25% LGO yield at 90 min obtained in the THF/H₂O (99/1) mixture is lower than the LGO yield (30.6% in 90 mins.) in pure THF. The much higher HMF yield in the presence of low concentrations of water (1 wt%) is attributed to HMF formed from the dehydration of glucose. Both soluble and insoluble humins are observed for reactions of both cellulose and LGA in both solvents systems.^{57,66}

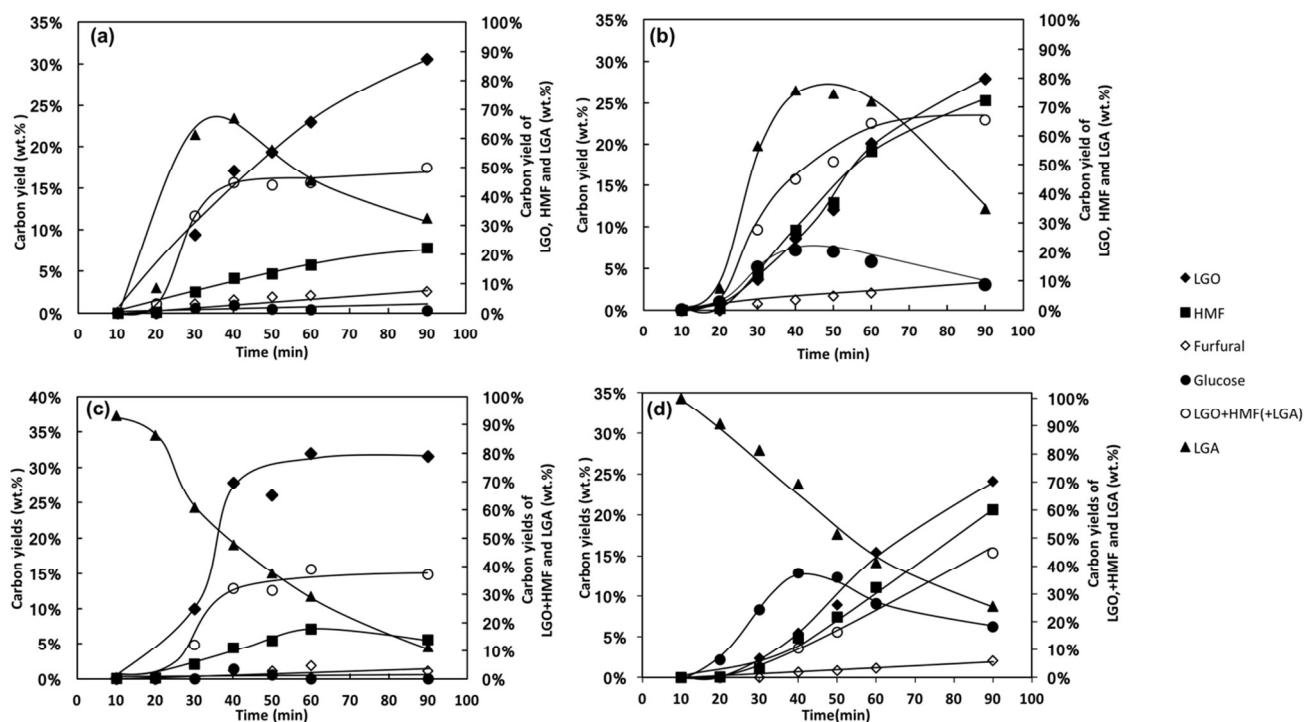


Figure 1 Influence of water on the conversion of (a) cellulose in pure THF (b) cellulose with 1 wt% H₂O in THF (c) LGA in pure THF (d) LGA with 1 wt% H₂O in THF. Reaction conditions: Cellulose (1 wt%, 0.53 g) or LGA (0.4 wt%, 0.2143 g), THF (60 mL), H₂SO₄ (24 μ L Conc., 7.5 mM), 1000 psi He, 170 $^{\circ}$ C, 700 rpm.

Figure 2 shows the stability of LGO in THF/H₂O mixtures with and without H₂SO₄. Approximately 33.6% of the LGO degrades in 60 mins with pure THF without an acid. Only trace amounts of HMF were observed in the HPLC during LGO conversion, suggesting that most of the LGO was converted into low volatility humins. The addition of 24 μ L H₂SO₄, decreased the LGO degradation to 10.9% in 60 mins. This result agrees with the work of Shafizadeh *et al.* who found that addition reactions of the C=C bond in LGO, which led to dimers, oligomers and humins, were catalyzed by bases (in the absence of acid).⁵⁴ HMF was detected only when water was added to the THF in yields from 1.3% with 12.5% LGO conversion to 2.0% with 30.1% LGO conversion. By increasing the initial water content from 1 wt% to 5 wt%, in the presence of H₂SO₄, the amount of LGO that degrades increases from 12.5% to 30.1% in 60 mins, respectively. In summary, acids stabilize LGO in THF, while water accelerates the degradation of LGO.

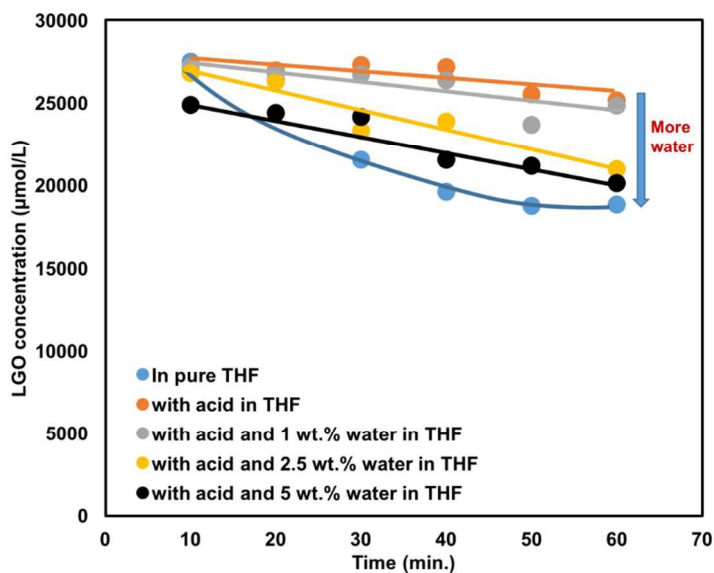


Figure 2 Influence of acid and water content on LGO degradation in THF. Reaction conditions: LGO (0.4 wt%, 0.2143 g), THF (60 mL), H₂SO₄ (24 μ L Conc., 7.5 mM), 1000 psi He, 170 $^{\circ}$ C, 700 rpm.

Effects of water content and cellulose loading on LGO and HMF production

Figure 3 shows the effect of the water content in the THF/water solvent and cellulose loading on the dehydration of cellulose in THF at 210 $^{\circ}$ C. The data in **Figure 3** are at the reaction time where the highest yields of LGO and HMF are obtained for each solvent composition. The reaction times for these maximum yields are listed in **Table S2**. The LGO yield decreases and the HMF yield increases (or goes through a maximum) with increasing water content in the solvent.

The yields of furfural, levulinic acid and formic acid typically decrease (or first go through a maximum then decrease) with increasing water content of the solvent.

Figure 4 shows the LGO and HMF yield as a function of time for cellulose conversion in a mixture of THF/H₂O (99/1). As shown in this figure, LGO and HMF are formed at the same time demonstrating that HMF is not a secondary product from LGO. In support of this conclusion, **Figure 5** shows the conversion of LGO in a mixture of THF/H₂O (99/1). There is only 5% yield HMF obtained with 40% conversion of LGO.

The yield of furfural from cellulose increases from 5.1% with pure THF to a maximum of 5.7% with 1 wt% water content and then gradually decreases to 3.3% with 10 wt% water content. The yields of LA and FA are constant at 2.1% and 0.7% regardless of the water content of the reaction media. The sum of the LGO, HMF and LGA yields reaches a maximum of 65% in the presence of 1 or 2.5% water content.

Increasing the cellulose loading from 1 to 10 wt% causes a decrease in the LGO and HMF yields. The higher concentrations of cellulose reactant generate higher concentrations of reactive intermediates, which oligomerize into humins. The HMF yield increases with increasing H₂O concentration, while the LGO yield decreases with increasing H₂O content at all cellulose loadings. The maximum combined yields of LGO, HMF and LGA decreased with increasing cellulose loading. These maximum combined yields were obtained in the presence of 1 - 2.5 wt% H₂O at all cellulose loadings. The furfural and FA yield is always around 5% and 1-2% respectively. The stability of THF is tested in the presence of 20 mM H₂SO₄ in THF with low concentration of water (1 wt.% H₂O) at 210 °C. Around 1-2 % THF degrades in 240 mins.

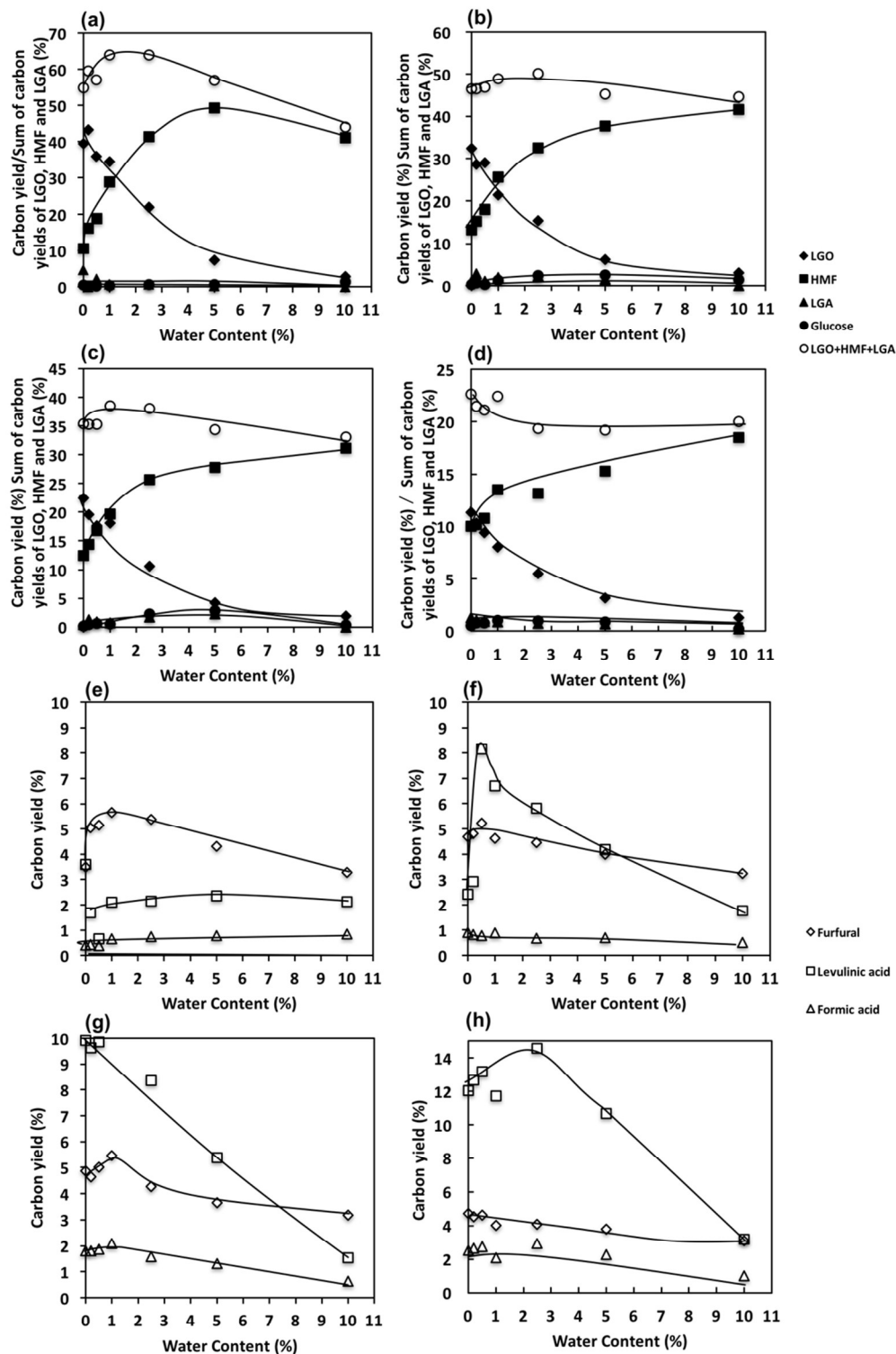


Figure 3 Influence of water content and cellulose loading on product yields for cellulose conversion. Reaction conditions: THF (60 mL), 210 °C, H₂SO₄ (64 μL Conc., 20 mM), 1000 psi H₂, 700 rpm. Cellulose loading: (a, e) 1 wt% (b, f) 3 wt% (c, g) 5 wt% (d, h) 10 wt%. Reaction time for the maximum yields of LGO and HMF are listed in **Table S2**.

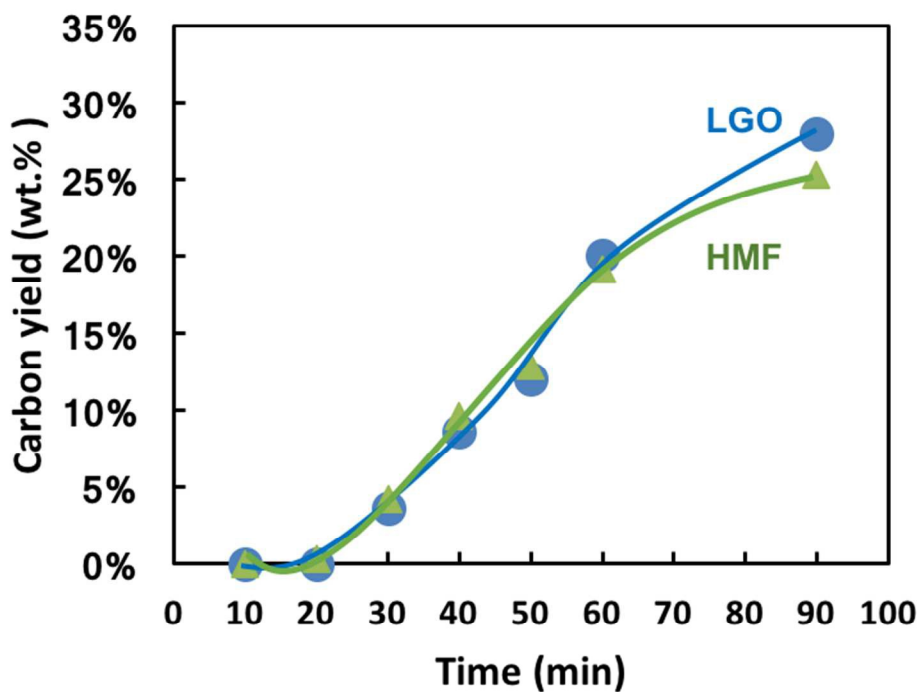


Figure 4 LGO and HMF yield during cellulose conversion in the presence of 1 wt% H₂O. Reaction conditions: Cellulose (1 wt%, 0.53 g), THF (60 mL), H₂SO₄ (24 μ L Conc., 7.5 mM), H₂O (1 wt%, 0.53 g), 1000 psi He, 170 $^{\circ}$ C, 700 rpm.

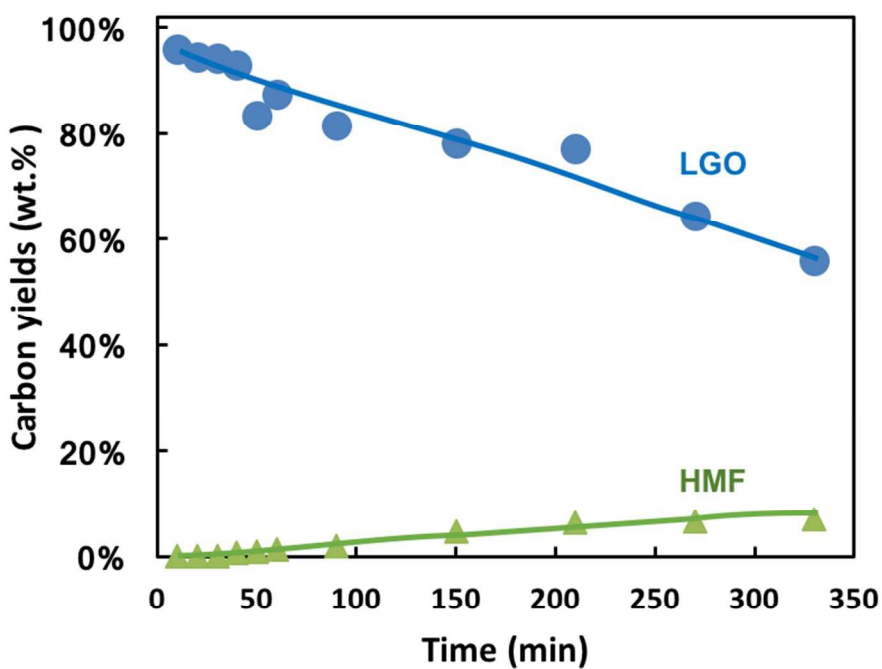


Figure 5 Conversion of LGO in the presence of 1 wt% H₂O in THF. Reaction conditions: LGO (0.4 wt%, 0.2143 g), THF (60 mL), H₂SO₄ (24 μL Conc., 7.5 mM), H₂O (1 wt%, 0.53 g), 1000 psi He, 170 °C, 700 rpm.

Kinetic solvent effects in the THF/water system

The marked shift in LGO/HMF selectivity as a function of water content is attributable to a) changes in the glucose/LGA equilibrium or b) changes in the rate of LGO isomerization to HMF (a water-mediated reaction). Having demonstrated that the latter is a negligible effect in the presence of dilute aqueous co-solvent, we now examine the role of water in the equilibrium-limited interconversion of glucose (HMF precursor) and LGA (precursor of LGO and HMF). As evidenced by **Figure 1**, the equilibrium between glucose and LGA develops quickly (<30 minutes) and is maintained throughout the entire course of the reaction. As the amount of water in the solvent system increases, the relative amounts of LGO and HMF precursors formed from cellulose change proportionally. **Table 3** compares the initial rates of LGO and HMF formation in THF/water mixtures to the equilibrium ratio of glucose to LGA in solution, which is constant throughout the reaction. If the change in HMF/LGO selectivity was only a function of the relative amounts of their chemical precursors in solution, then the initial rates of HMF and LGO production might scale accordingly. As shown in Table 3, however, the rate of HMF formation (relative to LGO formation) appears to increase with water content to a slightly greater extent than the ratio of glucose to LGA in solution. That is, a 37-fold increase in the ratio of glucose to LGA corresponds to a 53-fold increase in the ratio of the initial rates of HMF to LGO formation. This might be explained by the fact that LGA undergoes direct dehydration to HMF without needing to pass through glucose as an intermediate. However, we also note that the *combined* rate of HMF and LGO production increases by a factor of two as the water content of the solvent system increases from zero to 5 wt%. We interpret this to indicate that glucose not only becomes more abundant than LGA as water is added to the solvent system, but it becomes more reactive than LGA as well.

Table 3. Initial rates of HMF and LGO formation and equilibrium ratio of glucose to LGA concentrations as a function of water content.

wt% H ₂ O	$\left[\frac{C_{\text{glucose}}}{C_{\text{LGA}}} \right]_{\text{eq}}$	$r_{\text{initial}}^{\text{HMF}}$ (mmol hr ⁻¹)	L ⁻¹	$r_{\text{initial}}^{\text{LGO}}$ (mmol hr ⁻¹)	L ⁻¹	$r_{\text{initial}}^{\text{HMF}}/r_{\text{initial}}^{\text{LGO}}$	$r_{\text{initial}}^{\text{HMF}} + r_{\text{initial}}^{\text{LGO}}$
0	0.03	2.74		14.16		0.19	16.90
1	0.25	10.27		12.85		0.80	23.12
2.5	0.66	18.66		5.38		3.20	24.04
5	1.11	29.08		2.89		10.07	31.97

Reaction conditions: Cellulose (1 wt%, 0.53 g), THF (60 mL), H₂SO₄ (24 μL Conc., 7.5 mM), 1000 psi He, 170 °C, 700 rpm.

We note that glucose contains a greater number of hydroxyl groups than LGA, and the

interaction of these two species with water and THF molecules in THF/water mixtures would therefore be characterized by different energetics. Vlachos and co-workers demonstrated how preferential solvation of hydroxyl substituents by water molecules in 50/50 DMSO/water mixtures gives rise to an increased activity in the acid-catalyzed dehydration of fructose to yield HMF.⁶⁷ The details of how these types of solvent-solute interactions give rise to differences in the reactivity of glucose and LGA in THF/water mixtures are beyond the scope of this study. However, the fact that such dilute amounts of water in the THF solvent system induces large, solute-specific changes in reaction rates (and therefore selectivities) is of general significance from a process design standpoint, as will be demonstrated in the techno-economic analyses to follow.

System-level Studies for LGO and HMF production from cellulose

We first developed a process flow diagram (PFD) for the production of LGO and HMF from cellulose (shown in **Figure 6**), and then a process model, using Aspen Plus Process Simulator (V8.8 Aspen Technology), based on the experimental work in this publication. The cellulose feed (Stream 1) is mixed with fresh makeup H_2SO_4 (Stream 2) and THF solvent (Stream 12) from the THF accumulator (T-1) and supplied to the dehydration reactor (R-1), in which cellulose is converted to LGO, HMF, LGA, furfural, formaldehyde, LA, FA, and humins (the remainder of unconverted cellulose) at 170°C and 1000 psi. According to the experimental results, H_2SO_4 is loaded at 1/30 mass ratio of cellulose, and the yields of dehydration products from cellulose depends on the cellulose loading (wt% in THF) and water content (wt% in THF and cellulose) at the reactor throat (Stream 3). Both a water makeup stream (Stream 12) and a molecular sieve adsorber (S-3) are considered to maintain the desired water content. The H_2SO_4 remaining in the raw product stream (Stream 4) is then neutralized by slaked lime (Stream 5). The vapor fraction (Stream 7) of the neutralizer (R-2) product (Stream 6) is collected via a flash drum (S-1) and sent to T-1, while the remaining liquid and humin mixture (Stream 8) are separated in the filter (S-2). The humins (Stream 9) are burned to produce heat and electricity in the boiler/turbogenerator if necessary. The filtered liquid (Stream 10) feeds to the product distillation columns (D-1 and D-2), where a product stream containing LGO, HMF and LGA is obtained at the bottom (Stream 17) with over 99% recovery. To remove the soluble humins/oligomers, Stream 10 is first fed into the reboiler of D-1, where the high-boiling humins accumulate and are withdrawn from the reboiler bottom intermittently. The top product of D-1 (Stream 11) is mainly THF and water azeotrope, which is recycled back to T-1, while the top fraction from D-2 (Stream 16) is a mixture of excess water and other light components, such as LA, furfural, and FA. This stream can be sent to wastewater treatment or further processed if necessary. The base design is based on a cellulose feedstock rate of 17,000 kg/hr, which is equivalent to 1,000 dry tons of white birch per day.

We first simulate a “base case” design to obtain data that we then use to explore a wider range of operating conditions, using an optimization model. Specifically, we obtain sizing and cost data (parameters PC_0 , SV_0 , β , and γ) that can then be used to calculate the unit installed cost, IC , at different capacities (under different cellulose loading and water content) using the exponential scaling expression shown in Equation 1.

$$IC = \gamma PC_0 \left(\frac{SV}{SV_0} \right)^\beta \quad (1)$$

The definitions and values of parameters PC_0 , SV_0 , β , and γ are given in **Table 4** (in 2015 USD based on the Chemical Engineering Plant Cost Index).

Based on the installed equipment cost of each unit u , IC_u , calculated using Eq. (1), we first calculate the total capital investment, TCI , taking into account other direct and indirect costs via an additional cost factor ($ACF = 46\%$)⁶⁸ as described in Equation 2.

$$TCI = \frac{\sum_u IC_u}{(1-ACF)} \quad (2)$$

The TCI is then annualized using a capital charge factor, $CCF = 13.7\%$, calculated based on the parameters listed in Table S2⁶⁸. The yearly capital charge CC is shown in Equation 3.

$$CC = CCF \cdot TCI \quad (3)$$

The utility requirements of several unit operations, obtained from Aspen Plus simulations, are presented in **Table 4**. The utility cost and the raw material costs (for feedstock and makeup chemicals) form the overall variable operating costs. The fixed operating costs, including labor and various overhead items, are assumed to be a fraction (2.5%) of TCI .

Table 4. Capital costs (2015\$) and scaling factors for the main equipment*

Equipment	Base cost (\$) PC_0	Scaling value SV_0	Units	Scaling basis	Scaling factor β	Installed factor γ	Reference
R-1	48,658,000	601,902	kg/hr	feed	0.60	1.50	NREL ⁶⁸
R-2	1,377,000	602,330	kg/hr	feed	0.70	1.50	Aspen Plus
S-1	144,000	602,330	kg/hr	feed	0.70	2.00	Aspen Plus
S-2	8,151,000	11,631	kg/hr	solid feed	1.00	1.70	NREL ⁶⁸
S-3	285,000	16,856	kg/hr	adsorbed water	0.70	2.00	Aspen Plus
D-1	1,790,000	9,117	kmol/hr	vapor flow	0.60	2.40	Aspen Plus
D-2	538,000	129	kmol/hr	vapor flow	0.60	2.40	Aspen Plus
T-1	144,000	590,238	kg/hr	feed	0.70	2.00	Aspen Plus

* Cost parameters used for calculating capital charge factor are listed in **Table S4**.

Based on the process and the data obtained from Aspen Plus simulations, we formulated an optimization model to find the optimal combination of cellulose loading and water content. The

objective function was to minimize the unit production cost of the mixture of LGO, HMF and LGA (since they all can be converted to valuable C6 chemicals under similar conditions). A polynomial model was developed to fit the yields of cellulose dehydration products as a function of cellulose loading and water content. Material and energy balances were formulated for each equipment. The Underwood's method was used to model all distillation columns to capture the impact of feed composition on the column size and duty. The optimization model was used to simultaneously determine whether a water makeup stream (Stream 12) or molecular sieve adsorber (S-3) is required to maintain the optimal water content upon the feed (S-3) to dehydration reactor (R-1).

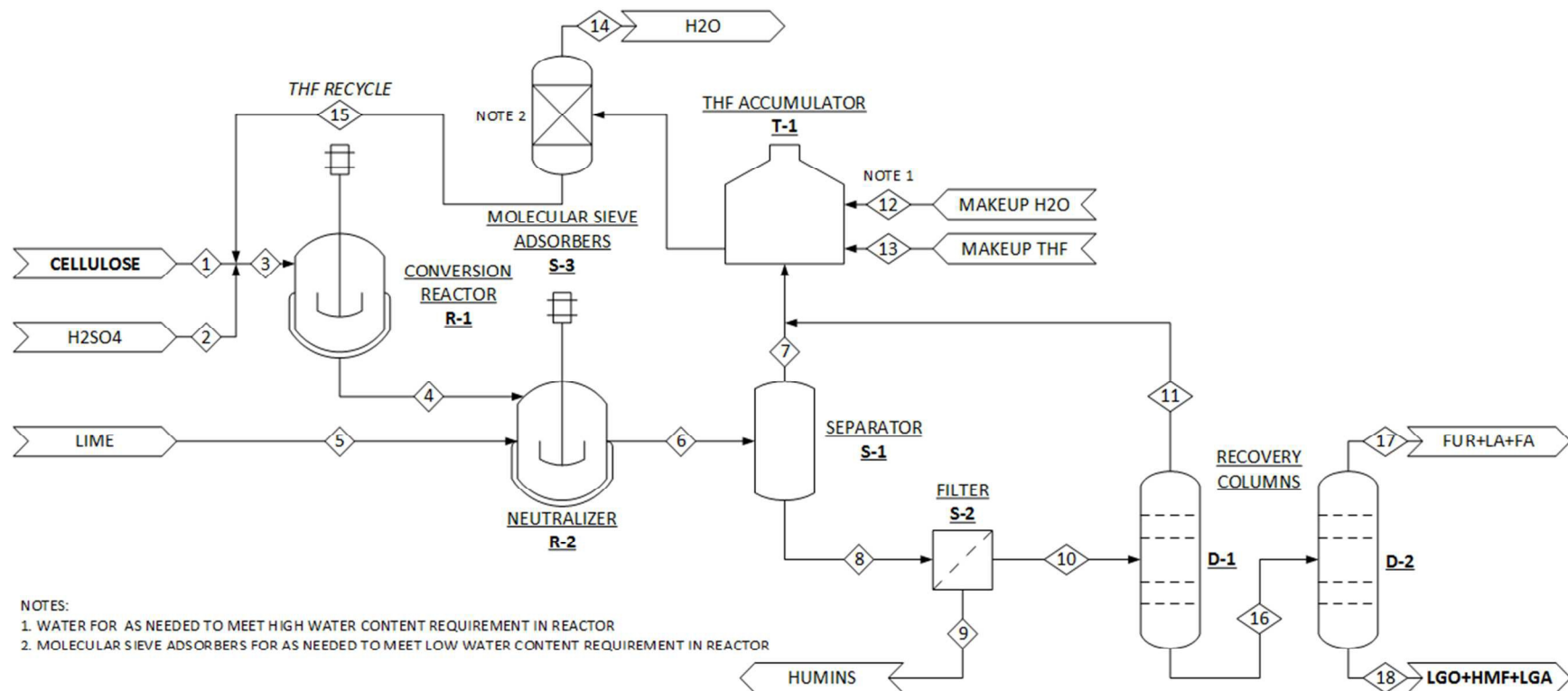


Figure 6. Overall process flow diagram

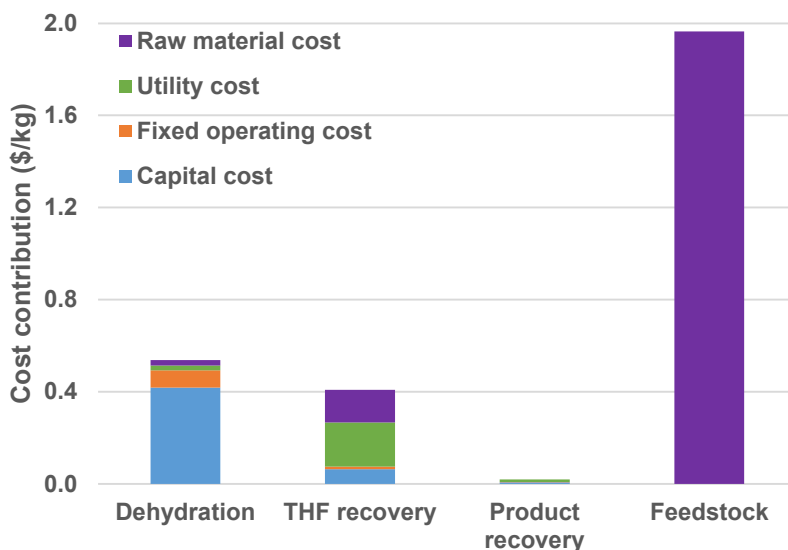


Figure 7. Cost contribution per process section (\$/kg product)

The optimal cellulose loading and water content were determined to be 2.2% and 1.9% respectively, leading to a production cost of the LGO, HMF and LGA mixture equal to \$2.93/kg. **Figure 7** illustrates the contribution of each process section to the overall production cost. The cellulose feedstock is the primary cost contributor (when purchased at \$0.825/kg), contributing \$1.96/kg of product or 67.1 % of the overall production cost. The next highest contributor is the dehydration section (\$0.54/kg, 14.3%) due to the capital expense associated with conversion of the dilute cellulose/solvent mixture. The THF recovery section is also a significant contributor due to utility costs (\$0.19/kg) for separation and makeup THF (\$0.14/kg). Since the feedstock cost weighs heavily on the overall production cost, it is further studied over a larger range of values (\$0-2.0/kg). **Figure 8** shows the minimum product cost and its associated optimal cellulose loading and water content as a function of cellulose price. We see that the cellulose loading decreases and the production cost increases, almost linearly, with cellulose price, while the optimal water content remains almost constant. If a relatively inexpensive cellulose (\$0.1/kg) is used, the minimum production cost decreases to \$1.0/kg, using a 4.0% cellulose loading. However, the optimal cellulose loading cannot be greater than 5.0%, regardless of the cellulose price, while the optimal water content stays between 1.8% and 1.9%.

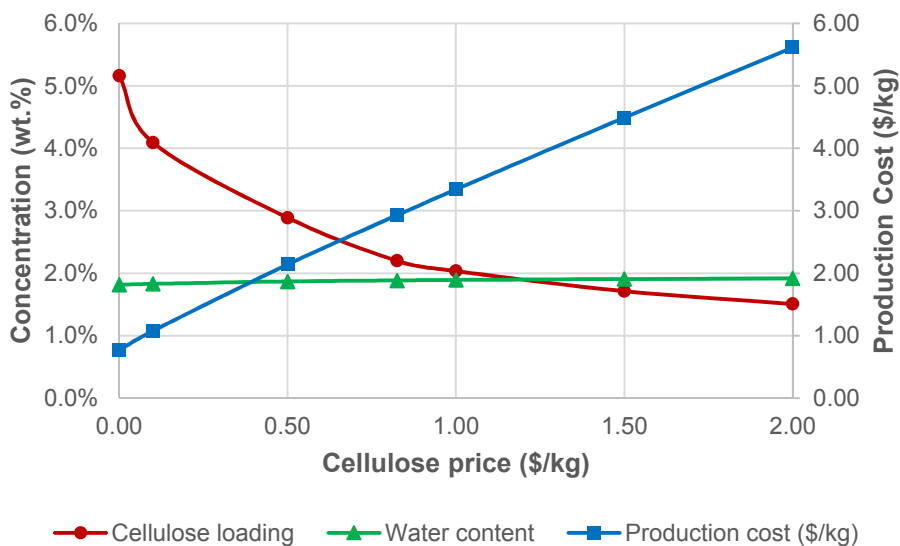


Figure 8. Optimal design scenarios as a function of cellulose price

Finally, a sensitivity analysis was performed to understand how the cellulose loading and water content impacts the economics. **Figure 9** shows the optimal production cost as a function of cellulose loading and water content. The point at the bottom left corner of the plot (2.2% cellulose loading with 1.9% water content) corresponds to the optimal design with cellulose price at \$0.825/kg, discussed previously. The results show that the production cost can vary from \$2.92/kg to \$8.20/kg, and that a wide range of cellulose loading and water content combinations can lead to a cost lower than \$3.00/kg. A high cellulose loading (>6.0%) leads to low product yields and therefore high unit production cost (>\$3.5/kg).

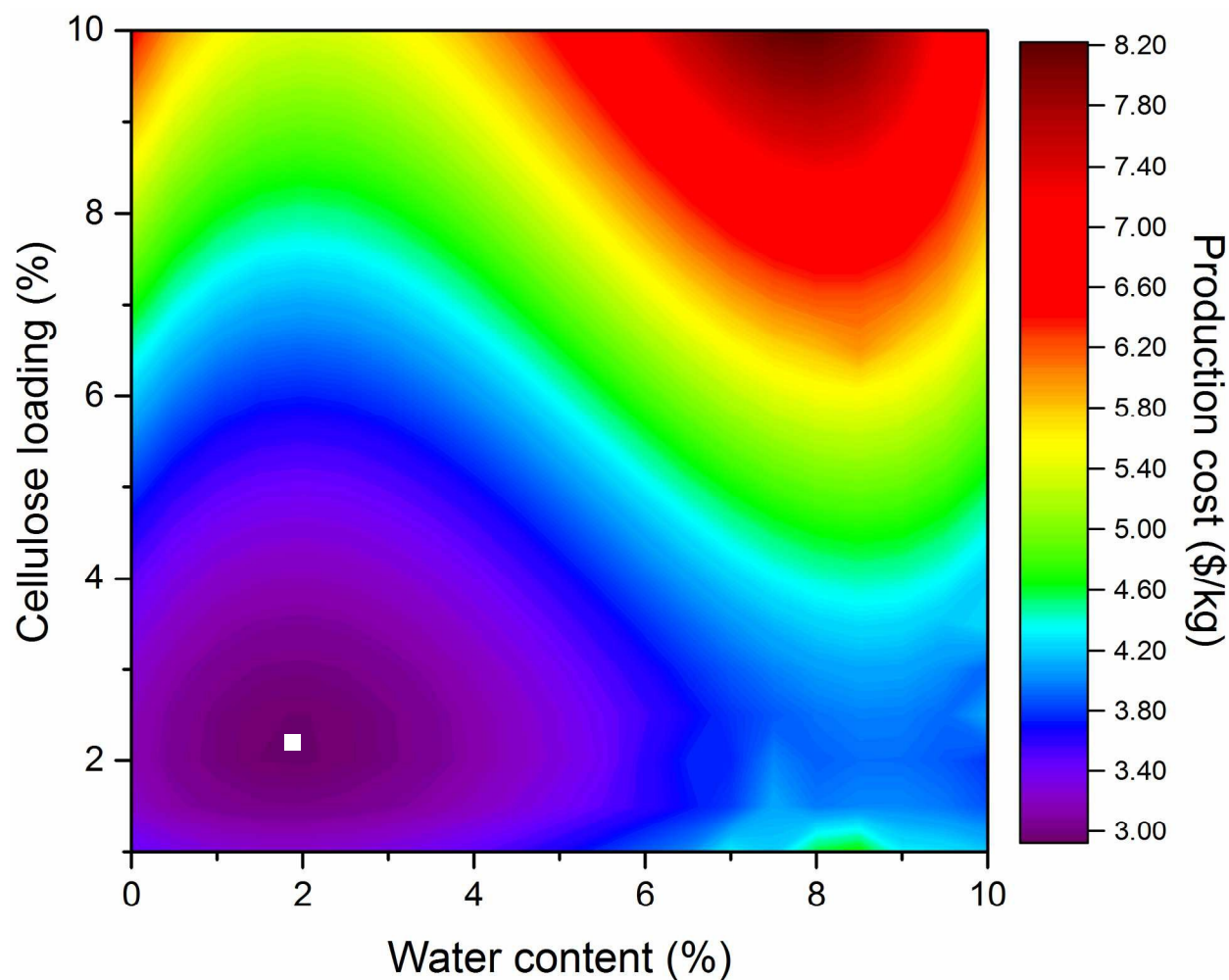


Figure 9. Production cost (\$/kg) as a function of cellulose loading and water content.

Conclusions

LGA is the primary product of acid catalyzed cellulose conversion in both pure THF, and in mixtures of THF with dilute water (<5 wt%). LGO and HMF are both produced via dehydration of LGA. Glucose undergoes dehydration to form HMF. The major sources of carbon loss in THF and in THF/water mixtures are oligomerization of glucose and LGO to form humins. Increasing the water content in the solvent (up to 5 wt%) increases the HMF selectivity, the glucose selectivity, and decreases the LGO selectivity. The ratio between glucose and LGA stays constant throughout the reaction demonstrating that this is an equilibrium-limited reaction. The increased HMF selectivity in the presence of low concentrations of H₂O (<5 wt%) is attributable to a) hydrolysis of LGA to yield glucose (an HMF precursor), and b) the enhanced reactivity of glucose compared to LGA in THF/water mixtures. The fact that glucose undergoes dehydration more readily than LGA in the presence of an aqueous co-solvent may be due to enhanced solvation of this hydrophilic substrate by water. LGO isomerization is a minor reaction pathway

for HMF formation at low water concentrations (<5wt%). Maximum combined yields of LGO and HMF and LGA (~65 carbon%) are achieved in the presence of 1- 2.5 wt% H₂O. Acid stabilizes LGO, while H₂O accelerates the degradation of LGO. LGO and HMF yields decrease with increased cellulose loadings.

The highest total yields of LGO and HMF obtained in this paper were with THF/H₂O mixture as the solvent. The rate of LGO and HMF degradation is lower in THF compared to the other organic solvents studied in this paper. The LGO/HMF yields increase with the increased strength of the acid catalyst tested in this study according to the following order HCOOH < H₃PO₄ < H₂SO₄.

The results of techno-economic analyses for LGO and HMF production from cellulose have shown that the overall production cost can vary from \$2.92/kg to \$8.20/kg, depending on cellulose loadings and the water content of the solvent system. Optimal process conditions with respect to these two variables are 2%~3% cellulose loading and 1.5~2.5% water content at production costs of less than \$3.00/kg.

Acknowledgement

This material is based upon work supported by the Department of Energy, Office of Energy Efficiency and Renewable Energy (EERE), under Award Number DE-EE0006878. Any opinions, findings, and conclusions or recommendations expressed in this material are those of the authors and do not necessarily reflect the views of the Department of Energy.

Reference:

- 1 M. Miura, H. Kaga, T. Yoshida, K. Ando, G. Dobele, T. Dizhbite, G. Rossinskaja, G. Telysheva, D. Meier, S. Radtke, O. Faix, Q. Lu, X. C. Yang, C. Q. Dong, Z. B. F. Zhang, X. M. Zhang, X. F. Zhu, J. Zandersons, A. Zhurinskaja, G. Dobele, V. Jurkjane, J. Rizhikovs, B. Spince, A. Pazhe, Q. Lu, X. M. Zhang, Z. B. F. Zhang, Y. Zhang, X. F. Zhu, C. Q. Dong, X. Wei, Z. Wang, Y. Wu, Z. Yu, J. Jin and K. Wu, *J. Anal. Appl. Pyrolysis*, 2011, **47**, 222–226.
- 2 S. Kudo, Z. Zhou, K. Yamasaki, K. Norinaga and J. Hayashi, *Catalysts*, 2013, **3**, 757–773.
- 3 S. Kudo, Z. Zhou, K. Norinaga and J. Hayashi, *Green Chem.*, 2011, **13**, 3306.
- 4 Q. Lu, X. ning Ye, Z. bo Zhang, C. qing Dong and Y. Zhang, *Bioresour. Technol.*, 2014, **171**, 10–15.
- 5 L. Nieva, A. Volpe and E. Laura Moyano, *Cellulose*, 2015, **22**, 215–228.
- 6 A. M. Sarotti, R. A. Spanevello and A. G. Suárez, *Green Chem.*, 2007, **9**, 1137.
- 7 F. Shafizadeh, R. H. Furneaux and T. T. Stevenson, *Carbohydr. Res.*, 1979, **71**, 169–191.
- 8 X. Sui, Z. Wang, B. Liao, Y. Zhang and Q. xiang Guo, *Bioresour. Technol.*, 2012, **103**, 466–469.
- 9 H. Kawamoto, S. Saito, W. Hatanaka and S. Saka, *J. Wood Sci.*, 2007, **53**, 127–133.
- 10 F. Cao, T. J. Schwartz, D. J. McClelland, S. H. Krishna, J. A. Dumesic and G. W. Huber, *Energy Environ. Sci.*, 2015, **8**, 1808–1815.
- 11 M. De bruyn, J. Fan, V. L. Budarin, D. J. Macquarrie, L. D. Gomez, R. Simister, T. J. Farmer, W. D. Raverty, S. J. McQueen-Mason and J. H. Clark, *Energy Environ. Sci.*, 2016, **9**, 2571–2574.
- 12 G. Dobele, G. Rossinskaja, G. Telysheva, D. Meier and O. Faix, *J. Anal. Appl. Pyrolysis*, 1999, **49**, 307–317.
- 13 Q. Lu, X. M. Zhang, Z. B. Zhang, Y. Zhang, X. F. Zhu and C. Q. Dong, *BioResources*, 2012, **7**, 2820–2834.
- 14 Q. Lu, X. C. Yang, C. Q. Dong, Z. F. Zhang, X. M. Zhang and X. F. Zhu, *J. Anal. Appl. Pyrolysis*, 2011, **92**, 430–438.
- 15 M. E. Zakrzewska, E. Bogel-Lukasik and R. Bogel-Lukasik, *Chem. Rev.*, 2011, **111**, 397–417.
- 16 J. N. Chheda, Y. Roman-Leshkov and J. a. Dumesic, *Green Chem.*, 2007, **9**, 342.
- 17 R. Weingarten, A. Rodriguez-Beuerman, F. Cao, J. S. Luterbacher, D. M. Alonso, J. A. Dumesic and G. W. Huber, *ChemCatChem*, 2014, **6**, 2229–2234.
- 18 T. Deng, X. Cui, Y. Qi, Y. Wang, X. Hou and Y. Zhu, *Chem. Commun.*, 2012, **48**, 5494.
- 19 H. Xia, S. Xu, X. Yan and S. Zuo, *Fuel Process. Technol.*, 2016, **152**, 140–146.
- 20 J. Yang, K. O. De Vigier, Y. Gu and F. Jérôme, *ChemSusChem*, 2015, **8**, 269–274.
- 21 Y. Roman-Leshkov, J. N. Chheda and J. A. Dumesic, *Science (80-.)*, 2006,

- 312**, 1933.
- 22 L. Atanda, A. Shrotri, S. Mukundan, Q. Ma, M. Konarova and J. Beltramini, *ChemSusChem*, 2015, **8**, 2907–2916.
- 23 L. Atanda, M. Konarova, Q. Ma, S. Mukundan, A. Shrotri and J. Beltramini, *Catal. Sci. Technol.*, 2016.
- 24 R. Rinaldi, R. Palkovits and F. Schüth, *Angew. Chemie - Int. Ed.*, 2008, **47**, 8047–8050.
- 25 J. B. Binder, J. B. Binder, R. T. Raines and R. T. Raines, *J. Am. Chem. Soc.*, 2009, **131**, 1979–85.
- 26 H. Zhao, J. E. Holladay, H. Brown and Z. C. Zhang, *Science (80-.)*, 2007, **316**, 1597–1600.
- 27 S. H. Krishna, D. J. McClelland, Q. A. Rashke, J. A. Dumesic and G. W. Huber, *Green Chem.*, 2017, **19**, 1278–1285.
- 28 Z. J. Wiczak, *Pure Appl. Chem.*, 1994, **66**, 2189–2192.
- 29 A. M. Sarotti, M. M. Zanardi, R. A. Spanevello and A. G. Suarez, *Curr. Org. Synth.*, 2012, **9**, 439–459.
- 30 V. Corne, M. C. Botta, E. D. V. Giordano, G. F. Giri, D. F. Llompert, H. D. Biava, A. M. Sarotti, M. I. Mangione, E. G. Mata, A. G. Suárez and R. A. Spanevello, *Pure Appl. Chem.*, 2013, **85**, 1683–1692.
- 31 J. Sherwood, M. De bruyn, A. Constantinou, L. Moity, C. R. McElroy, T. J. Farmer, T. Duncan, W. Raverty, A. J. Hunt and J. H. Clark, *Chem Commun*, 2014, **50**, 9650–9652.
- 32 P. Werle, M. Morawietz, S. Lundmark, K. Sörensen, E. Karvinen and J. Lehtonen, in *Ullmann's Encyclopedia of Industrial Chemistry*, 2008, pp. 263–281.
- 33 C. Moreau, M. Naceur and A. Gandini, *Top. Catal.*, 2004, **27**, 11–30.
- 34 A. J. Domb, J. Kost and D. M. Wiseman, *Handbook of Biodegradable Polymers*, 1998.
- 35 R. W. Tess, R. D. Harline and T. F. Mika, *Ind. Eng. Chem.*, 1957, **49**, 374–378.
- 36 P. Daorattanachai, S. Namuangruk, N. Viriya-empikul, N. Laosiripojana and K. Faungnawakij, *J. Ind. Eng. Chem.*, 2012, **18**, 1893–1901.
- 37 S. Yin, Y. Pan and Z. Tan, *Int. J. Green Energy*, 2011, **8**, 234–247.
- 38 B. F. M. Kuster, *Starch-Starke*, 1990, **42**, 314–321.
- 39 Y. J. Pagan-Torres, T. Wang, J. M. R. Gallo, B. H. Shanks and J. A. Dumesic, *ACS Catal.*, 2012, **2**, 930–934.
- 40 C. M. Cai, N. Nagane, R. Kumar and C. E. Wyman, *Green Chem.*, 2014, **16**, 3819–3829.
- 41 C. M. Cai, T. Zhang, R. Kumar and C. E. Wyman, *Green Chem.*, 2013, **15**, 3140.
- 42 Y. Tsutsumi, A. Nishikata and T. Tsuru, *Corros. Sci.*, 2007, **49**, 1394–1407.
- 43 Y. Su, H. M. Brown, X. Huang, X. dong Zhou, J. E. Amonette and Z. C. Zhang, *Appl. Catal. A Gen.*, 2009, **361**, 117–122.
- 44 K. M. Rapp, *Process for preparing pure 5-hydroxymethylfurfuraldehyde*, Google Patents, 1988.

- 45 M. Bicker, J. Hirth and H. Vogel, *Green Chem.*, 2003, **5**, 280–284.
- 46 A. I. Torres, P. Daoutidis, M. Tsapatsis, M. Woo, C. A. Floudas, M. von Keitz, K. J. Valentas, J. Wei and M. Tsapatsis, *Energy Environ. Sci.*, 2010, **3**, 1560.
- 47 F. K. Kazi, A. D. Patel, J. C. Serrano-Ruiz, J. A. Dumesic and R. P. Anex, *Chem. Eng. J.*, 2011, **169**, 329–338.
- 48 A. I. Torres, M. Tsapatsis and P. Daoutidis, *Comput. Chem. Eng.*, 2012, **42**, 130–137.
- 49 W. Liu, F. Richard Zheng, J. Li and A. Cooper, *AIChE J.*, 2014, **60**, 300–314.
- 50 A. Mukherjee, M.-J. Dumont and V. Raghavan, *Biomass and Bioenergy*, 2015, **72**, 143–183.
- 51 R.-J. van Putten, J. C. van der Waal, E. de Jong, C. B. Rasrendra, H. J. Heeres and J. G. de Vries, *Chem. Rev.*, 2013, **113**, 1499–1597.
- 52 Y. Lin, J. Cho, G. a Tompsett, P. R. Westmoreland and G. W. Huber, *Cellulose*, 2009, 20097–20107.
- 53 R. Vinu and L. J. Broadbelt, *Energy Environ. Sci.*, 2012, 9808–9826.
- 54 F. Shafizadeh, R. H. Furneaux and T. T. Stevenson, *Carbohydr. Res.*, 1979, **71**, 169–191.
- 55 S. Helle, N. M. Bennett, K. Lau, J. H. Matsui and S. J. B. Duff, *Carbohydr. Res.*, 2007, **342**, 2365–2370.
- 56 M. Käldestrom, N. Kumar, T. Heikkilä, M. Tiitta, T. Salmi and D. Y. Murzin, *ChemCatChem*, 2010, **2**, 539–546.
- 57 X. Hu, L. Wu, Y. Wang, D. Mourant, C. Lievens, R. Gunawan and C.-Z. Li, *Green Chem.*, 2012, **14**, 3087.
- 58 L. Qi, Y. F. Mui, S. W. Lo, M. Y. Lui, G. R. Akien and I. T. Horváth, *ACS Catal.*, 2014, **4**, 1470–1477.
- 59 E. I. Gürbüz, J. M. R. Gallo, D. M. Alonso, S. G. Wettstein, W. Y. Lim and J. A. Dumesic, *Angew. Chemie - Int. Ed.*, 2013, **52**, 1270–1274.
- 60 S. H. Krishna, T. W. Walker, J. A. Dumesic and G. W. Huber, *ChemSusChem*, 2017, **10**, 129–138.
- 61 I. M. Kolthoff, M. K. Chantooni and S. Bhowmik, *J. Am. Chem. Soc.*, 1968, **90**, 23–28.
- 62 I. M. Kolthoff and M. K. Chantooni, *J. Am. Chem. Soc.*, 1968, **90**, 5961–5964.
- 63 K. R. Enslow and A. T. Bell, *ChemCatChem*, 2015, **7**, 479–489.
- 64 G. Marcotullio and W. De Jong, *Carbohydr. Res.*, 2011, **346**, 1291–1293.
- 65 G. Marcotullio and W. De Jong, *Green Chem.*, 2010, **12**, 1739.
- 66 D. M. Alonso, S. G. Wettstein and J. A. Dumesic, *Green Chem.*, 2013, **15**, 584.
- 67 S. H. Mushrif, S. Caratzoulas and D. G. Vlachos, *Phys. Chem. Chem. Phys.*, 2012, **14**, 2637.
- 68 R. Davis, L. Tao, C. Scarlata, E. C. D. Tan, J. Ross, J. Lukas and D. Sexton, *Process Design and Economics for the Conversion of Lignocellulosic Biomass to Hydrocarbons: Dilute-Acid and Enzymatic Deconstruction of Biomass to Sugars and Catalytic Conversion of Sugars to Hydrocarbons NREL/TP-5100-62498*, 2015.